# FABRICATION AND CHARACTERIZATION OF HORIZONTALLY-ALIGNED CARBON NANOTUBE/SILICON CARBIDE NANOCOMPOSITE LAMINATES WITH ULTRA-HIGH NANOFIBER VOLUME FRACTION

Shaan Jagani[1], Jingyao Dai[1], Luiz Acauan[1], and Brian L. Wardle[1,2*]

[1] *Department of Aeronautics and Astronautics, Massachusetts Institute of Technology, Cambridge, MA, 02139*

[2] *Department of Mechanical Engineering, Massachusetts Institute of Technology, Cambridge, MA, 02139*

*Corresponding Author: wardle@mit.edu

**Keywords:** Carbon nanotubes, ceramic matrix composite, silicon carbide, nanoindentation, polymer infiltration and pyrolysis

## ABSTRACT

**Carbon nanotubes (CNTs) have gained considerable attention as potential nano-scale reinforcements in ceramic matrix composites (CMCs) due to their exceptional mechanical properties. The bulk nanocomposite laminating process for CMCs (BNL4CMC) was developed to make dense SiC/CNT composites with high-volume fractions of horizontally-aligned CNTs (HA-CNTs). The processing parameters were refined to establish new process-structure-property relationships, and the resulting composites were characterized using various techniques. X-ray microcomputed tomography confirmed the absence of micro/macro-scale porosity in the composites. Polarization studies using Raman spectroscopy demonstrated the anticipated alignment of CNTs in the laminates. Scanning electron microscopy images showed changes in the local microstructure, including the presence of nano-scale inclusions at the interface between nanofibers and the SiC matrix. X-ray diffraction confirmed the crystallinity of CNTs and the presence of a β-SiC phase within the crystallized composites. Mechanical characterization through nanoindentation revealed evolving mechanical properties throughout the processing stages, with the crystallized laminates exhibiting increased stiffness compared to the pyrolyzed and cured counterparts. However, the stiffness of the SiC/CNT composites was lower compared to polymer-infiltration-and-pyrolysis-derived SiC, suggesting the presence of nano-scale porosity in the SiC matrix. Thermogravimetric analysis of the cured laminates indicated anomalous weight loss, potentially due to the interaction between CNTs and the polymer matrix during the curing process. Further investigation is needed to understand the underlying mechanisms and optimize the curing process. Overall, this study successfully replicated and extended previous work in manufacturing SiC/CNT ceramic composites. The findings provide valuable insights into the synthesis, characterization, and behaviour of SiC/CNT laminates, paving the way for the development of tough and high-strength reinforced ceramics for various high-performance applications.**

## 1 INTRODUCTION

The mechanical properties of crystalline nanofibers like carbon nanotubes (CNTs) have garnered significant attention as potential nano-scale reinforcement for many material systems [1]. Their remarkable stiffness, strength, and high aspect ratio are comparable to those of reinforcing fibers currently utilized in ceramic matrix composites (CMCs) - exploiting these properties have resulted in enhanced toughness and superior crack resistance over conventional technical ceramics [2]. Moreover, the thermal and electrical properties of a resulting CNT-based composite enable multifunctionality in

applications such as sensing and thermal protection, making them particularly useful in demanding environments like space and hypersonic flight [3, 4].

Silicon carbide (SiC) is a widely studied and popular ceramic with good oxidation resistance, thermal stability, and mechanical properties [5]. These traits complement the properties of CNTs for potential applications, which motivated its use as the ceramic of choice for this work.

This study builds upon the previously introduced bulk nanocomposite laminating process for ceramic matrix composites (BNL4CMC) [6] process to produce and characterize dense, void-free crystalline SiC/CNT ceramic composites. Polymer-infiltration and pyrolysis (PIP) following a novel "knock-down" procedure on as-grown vertically-aligned CNTs (VA-CNT) is used to produce ceramic composites with a high-volume fraction of horizontally- aligned CNTs (HA-CNTs) [6]. Refinement of the processing parameters suggests new process-structure-property relationships as evidenced by micro-scale mechanical and chemical characterization of 4-ply composite samples. Scanning electron microscopy, micro-computed tomography, and x-ray diffraction were used to probe the microstructure and crystallinity of the composites at various stages of processing. Nanoindentation was used to determine the evolution of hardness and modulus throughout processing. Thermogravimetric analysis of the polymerized samples was intended to reveal the volume percent of CNTs. However, observations from nanoindentation and thermogravimetric analysis revealed variations in anticipated properties, suggesting the need for optimization in processing parameters. These findings will motivate further development of a reliable manufacturing process and an optimized SiC/CNT composite system.

## 2 MATERIALS AND METHODS

Vertically-aligned CNTS (VA-CNTs) were prepared using a chemical vapor deposition (CVD) process described in previous work [7-9]. 500 nm tall VA-CNT forests were produced on 3 cm x 4 cm silicon wafers coated with a 10 nm layer of $Al_2O_3$ and 1 nm of Fe via e-beam deposition [10]. Previous characterization work indicates these CNTS are multi-walled with an average diameter of 8 nm and an as-grown density of ~1.6 g/cm$^3$, 0.7% volume density, and 60-80 nm inter-CNT spacing [11-12].

The BNL4CMC process introduced in previous work [6] was reproduced to create 4-ply nanocomposite laminates for characterization, as depicted in **Figure 1**.

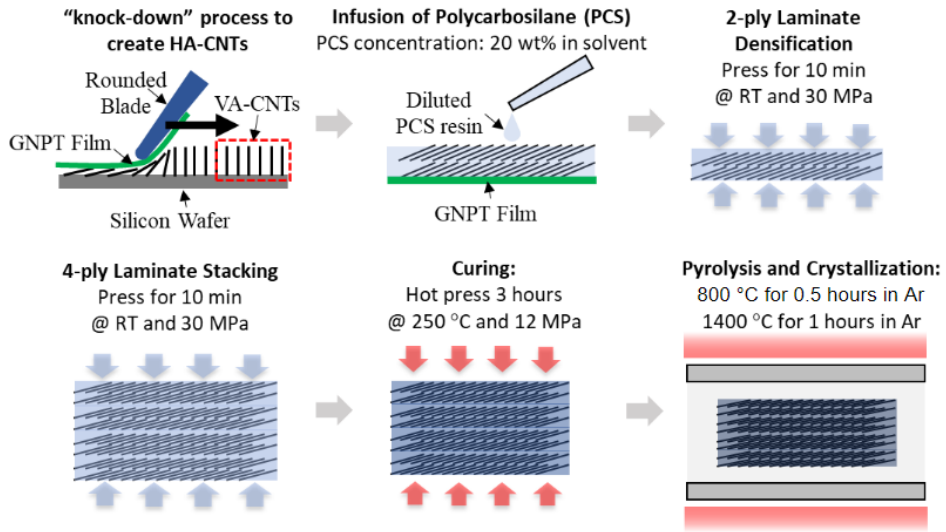


**Fig. 1 Schematic of the bulk nanocomposite laminating process for ceramic matrix composites (BNL4CMCs) [6]**

Densification and horizontal alignment of the CNTs was reproduced using a documented "knock-down" process [13]. A film of non-porous teflon (GNPT) is placed over as-grown VA-CNTs and a rounded blade is pressed and slid over the top to "knock-down" the forest, creating a densified 1-ply that preferentially adheres to the GNPT. This is repeated with a second forest to create densified, horizontally-aligned, and symmetric CNT (HA-CNT) 2-ply films ready for polymer infiltration.

Ceramic BNL samples were created using a PIP procedure previously developed for use with commercially available polycarbosilane (PCS, Starfire SMP-10) precursor resin [6]. Dry HA-CNT laminates were coated with a 15 wt% solution of SMP-10 and hexane for 60 seconds before removal of the excess resin via spin coating at 4000 rpm for 30 sec [6]. Removal of the solvent was achieved with a 12-hour drying step under vacuum before curing. The 2-ply HA-CNT laminates were densified in a hot-press under 30 MPa at room temperature for 10 min before being stacked together. This 4-ply laminate was cured at 250 °C for 3 hours at 12 MPa [6].

The resulting polymerized samples were pyrolyzed to convert the PCS matrix to SiC [6]. The cured samples were pyrolyzed in an inert gas tube furnace in argon (Ar) at 1 atm at 800 °C for 0.5 hours at a 4 °C /min heating rate and left to cool naturally [6, 14], in a comparable manner to previous work. These pyrolyzed samples were then further heat treated at 1400 °C in Ar for 1 hour with a 4 °C/min heating rate and 2 °C/min cooling rate to crystallize the as-pyrolyzed, amorphous SiC matrix. To mitigate the potential warping of the HA-CNT laminates and to serve as sacrificial oxidation material in the event of oxygen exposure, the samples were interposed between graphite plates during all heat treatments.

Analogously to previous work [6], microstructural characterization of the cured, pyrolyzed, and crystallized HA-CNT composites was achieved using scanning electron microscopy (SEM, Zeiss Sigma 300 VP) to inspect the fracture surfaces of hand-fractured samples and microcomputed tomography (µCT, Zeiss Xradia 520 Versa X-ray microscope) with an 80 kV source voltage and a voxel size of ~0.75 µm to assess micro-scale porosity. Thermogravimetric analysis (TGA, TA Instruments TGA 5500) of the as-cured samples was conducted to determine the volume fraction of CNTs in the cured, densified laminates. Polarized Raman spectroscopy (Renishaw) with a 532 nm source was used to conduct polarization experiments to verify CNT alignment. X-ray Diffraction (XRD, Rigaku Smartlab Multipurpose Diffractometer) was performed on HA-CNT laminates at each stage of processing to confirm emergent SiC crystallinity in the as-crystallized samples.
Mechanical characterization was performed via nanoindentation (Hystiron TI950 TriboIndenter) to determine the reduced elastic modulus and hardness of the cured, pyrolyzed, and crystallized laminates in both the axial (parallel to CNT) and transverse directions.

## 3 RESULTS AND DISCUSSION

The BNL process enabled manufacture of dense 4-ply ceramic matrix laminates with minimal warpage. X-ray microcomputed tomography of the laminates indicate apparent shrinkage in the out-of-place direction, with the as-cured sample measuring ~50 µm in thickness and the as-crystallized sample measuring ~25 µm without apparent micro/macro-scale porosity (see **Figure 2**). The degree of shrinkage has notably increased over previous work [6], potentially due to a smaller initial concentration of SMP-10 used in the precursor solution and modifications to the pyrolysis and crystallization procedure. The reduction in resin concentration was implemented to mitigate the occurrence of "crushing" of the laminates during the hot-pressing process due to non-uniform pressure distribution.

Polarization studies conducted via Raman spectroscopy confirm CNT alignment as anticipated from previous work [6]. Due to the orientation-dependent Raman intensity of the D band in CNTs [15], the Raman spectra of CNTs with different angles of light polarization can be used to illustrate the degree of nanotube alignment. **Figure 2(b)** depicts the integrated D-peak intensity (1246 $cm^{-1}$ to 1436 $cm^{-1}$) of the cured, pyrolyzed, and crystallized laminate Raman spectra as a function of polarization angle from 60° to 540°. The apparent 180° period of the resulting curves confirms two-fold symmetry of the laminate, indicating that the BNL4CMC process reproducibly enables the manufacture of nanocomposite laminates with horizontally-aligned CNTs. Phase shift between the laminate spectra is due to inconsistent sample alignment between polarization experiments.

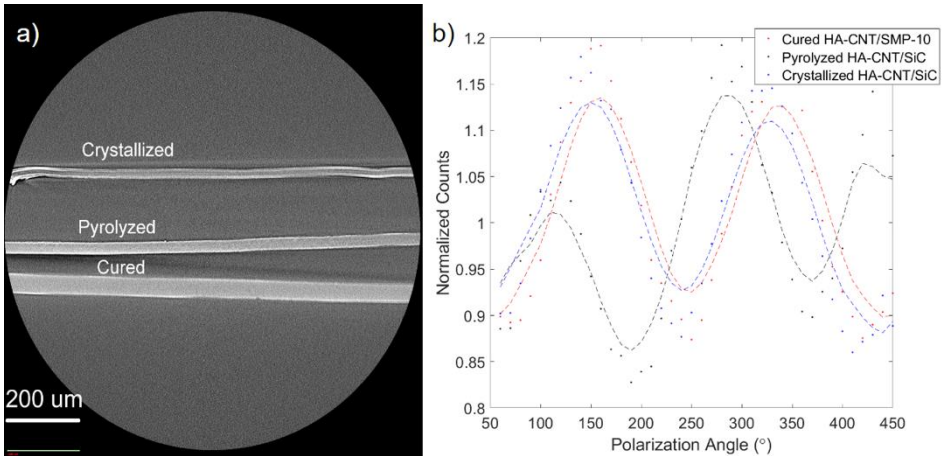


**Fig. 2 HA-CNT nanocomposite porosity and fiber alignment: (a) µCT of laminates at various stages of processing; (b) normalized counts of Raman CNT D-peak (smoothed to highlight periodicity) as a function of laser polarization angle.**

**Figure 3(a-e)** depicts SEM images of hand-fractured surfaces for laminates at each stage of processing. Higher resolution images of the pyrolyzed and crystallized samples in **Figure 3(d-e)** show exposed nanofibers and conspicuous changes in the local microstructure. Nano-scale inclusions are observable at the base of exposed nanofibers in the crystallized laminate in **Figure 3(e)** that are absent from the pyrolyzed fracture surface. Further investigation is necessary to validate the composition and structure of these inclusions. One plausible hypothesis is the occurrence of nanoscale grains nucleating at the interface between nanofibers and the matrix during the crystallization heat treatment, wherein their size is limited by the spacing between adjacent fibers.

X-ray diffraction was performed on the laminates, and subsequent peak matching substantiated the crystallinity of carbon nanotubes (CNTs) and the presence of a β-SiC phase within the crystallized sample. The experimental setup employed Bragg-Brentano geometry and a 1°/min scanning process ranging from 10° to 90° 2θ for each sample, as depicted in **Figure 3(f)**. The identified peaks corresponded to three diffractive modes of β-SiC, aligning with those observed in β-SiC nanopowders [16]. The observed increase in diffracted intensity corresponding to the carbon nanotubes (CNTs) is ascribed to the laminate density. Per previous work [6], the crystallized laminates exhibit higher density compared to the pyrolyzed sample, and correspondingly, the pyrolyzed laminates possess greater density than the cured laminate.

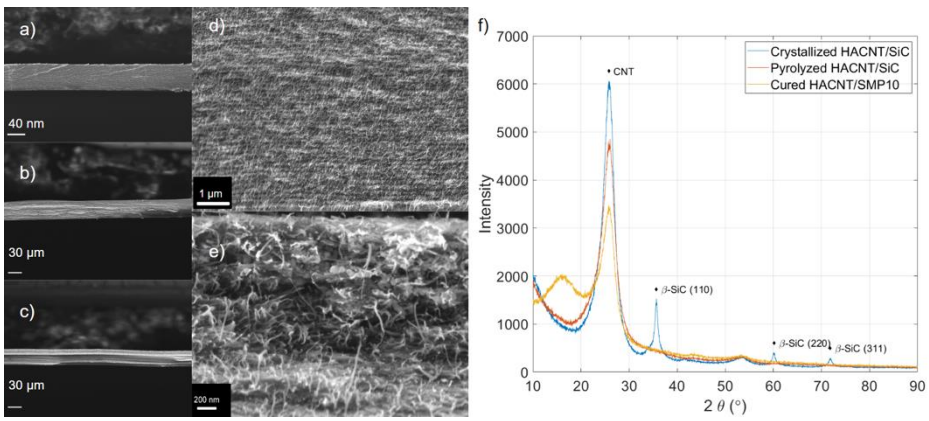


**Fig. 3 HA-CNT nanocomposite microstructure: (a-e) images of (a) as-cured, (b, d) pyrolyzed, and (c, e) crystallized 4-ply HA-CNT/SiC nanocomposite laminates; (f) XRD scan of 4-ply HA-CNT nanocomposite laminates at different fabrication stages.**

Previous work [6] cursorily explored the mechanical properties of amorphous HA-CNT/SiC laminates via nanoindentation. **Figure 4** depicts curve-fitted hardness and elastic modulus values for

cured, pyrolyzed, and crystallized laminates in both the axial and transverse directions to characterize mechanical anisotropy and microstructure evolution. Laminates were delicately retained with plastic clips before being vertically cold-mounted in 1.5" diameter acrylic pucks, which were ground and polished with SiC pads, diamond grit, and finally 0.05 um alumina particles in suspension to produce a surface suitable for nanoindentation. 20 quasi-static indentations using a trapezoidal loading curve (10 mN peak load for 5 seconds, 2 mN/s loading and unloading) and Berkovich tip were performed per sample orientation. The reduced modulus $E_R$ and hardness derived per Oliver and Pharr [17] are plotted in **Figure 4(b)**, showing increased stiffness for the crystallized laminates over the pyrolyzed and cured counterparts, but significantly reduced stiffness compared to neat SiC derived from similar PIP processes [18, 19], as encountered in previous work [6]. This is presumed to be due to the presence of nano-scale porosity in the SiC matrix and warrants further investigation. The study identified distinct groupings for laminates at different stages of processing. However, due to challenges in accurately distinguishing orientation effects from potential errors during sample preparation or mislabeling, clear conclusions regarding CNT orientation could not be confidently drawn.

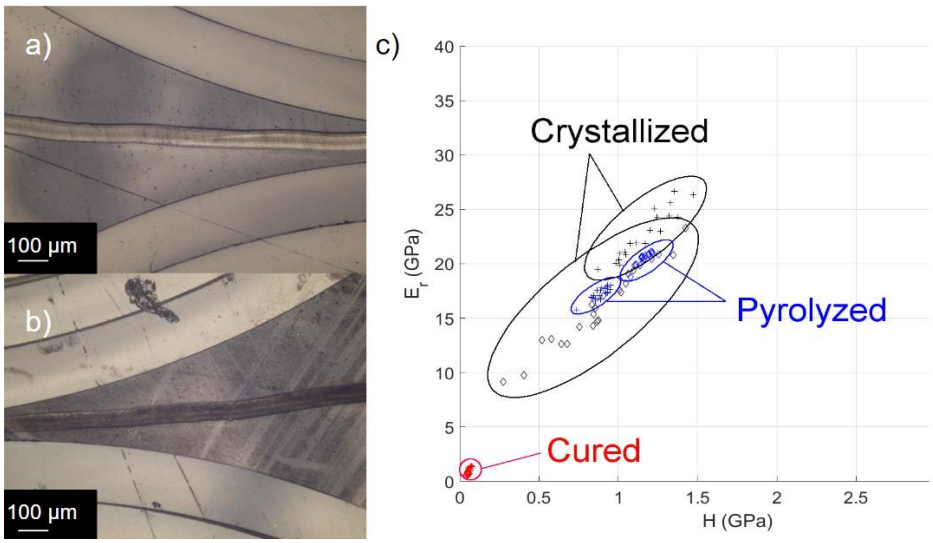


**Fig. 4 Nanoindentation: (a, b) optical images of polished (a) pyrolyzed and (b) crystallized laminates sandwiched between plastic sample clips; (c) Plotted reduced modulus and hardness values derived from quasi-static nanoindentation in both principal material directions.**

In previous work [6], thermogravimetric analysis in $N_2$ was employed to assess CNT volume percent and ceramic yield. This approach compared the weight loss of neat SMP-10 to that of CNT laminates - since CNTs exhibit thermal stability in an inert gas environment over the tested temperature, the fractional weight loss observed during TGA indicated the mass percentage of CNTs present in the sample. **Figure 5** depicts weight loss experiments for neat SMP-10 and recent fabricated laminates where anomalous weight loss patterns are apparent. The neat polymer exhibited mass loss of 22.6 - 24.6 wt%, while the cured laminates exhibited mass loss from 31.5 - 34.8 wt%. King et al. [20] suggest incomplete curing of the SMP-10 in the HA-CNT laminates could result in the retention of low-molecular-weight oligomers, which would affect mass loss during TGA. However, additional vacuum curing at 200C for 12 hours after hot pressing resulted in a negligible decrease in mass loss, suggesting a potential inhibitory effect of CNTs on the proper curing process of the polymer. These findings highlight the need for further investigation to understand the underlying mechanisms and interactions between CNTs and the polymer matrix.

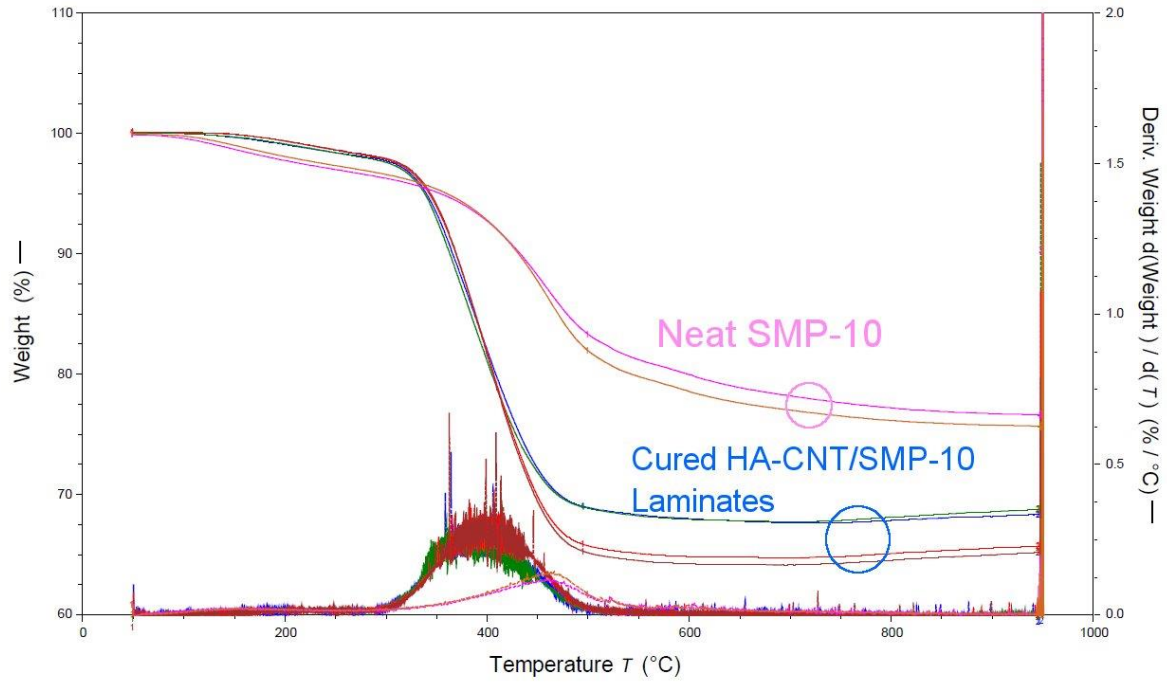


**Fig. 5 TGA of cured HA-CNT/SMP-10 laminates and neat, cured SMP-10**

## 4 CONCLUSIONS

In conclusion, the methods employed in this study successfully replicated and extended upon previous work in the manufacture and characterization of high-volume fraction HA-CNT/SiC ceramic matrix composites. The bulk nanocomposite laminating process for ceramic matrix composites (BNL4CMC) was reproduced and allowed for the creation of dense 4-ply ceramic matrix laminates with minimal warpage. Subsequent characterization and analysis revealed notable findings, such as apparent shrinkage in the out-of-place direction and the presence of nano-scale inclusions in the crystallized laminates. Polarization studies confirmed the alignment of CNTs in the laminates, while X-ray diffraction substantiated the presence of a β-SiC phase. Mechanical characterization through nanoindentation demonstrated evolving mechanical properties throughout the stages of processing, with distinct trends observed for the laminates at each stage. Furthermore, thermogravimetric analysis revealed anomalous weight loss patterns in the cured laminates, indicating a potential inhibitory effect of CNTs on the proper curing process of the polymer matrix.

These results and observations raise important questions and areas for further investigation. The deviations in shrinkage behavior and the presence of nano-scale inclusions in the crystallized laminates will be further scrutinized to understand the effect of high-volume fraction nanofibers on SiC crystallization. Reproduction of the nano-mechanical testing is also important to determine the discrepancy between measured values and other PIP-derived SiC, as well as confirm anisotropy with respect to CNT fiber alignment orientation. Additional testing to characterize fracture toughness and macro-scale elastic modulus is planned.

Chiefly, the anomalous weight loss observed in the cured laminates may suggest an interplay between the CNTs and the polymer matrix during the curing process. Follow-up TGA of HA-CNT laminates fabricated under various processing conditions will be conducted to understand the underlying mechanisms. Overall, this study provides valuable insights into the synthesis, characterization, and behavior of HA-CNT/SiC laminates, providing the basis for manufacture of tough, high-strength reinforced ceramics.

## ACKNOWLEDGEMENTS

This work was partially supported by the U.S Office of Naval Research (ONR) under grant/contract number N00014-22-1-2203, partially supported by the U.S. Army Research Laboratory and the U.S. Army Research Office through the Institute for Soldier Nanotechnologies (ISN) under contract number W911NF-13-D-0001, and partially supported by Airbus, ANSYS, Boeing, Embraer, Lockheed Martin, Saab AB, and Teijin Carbon America through MIT's Nano-Engineered Composite aerospace STructures (NECST) Consortium. This material is based upon work supported in part by the U. S. Army Research Office through the Institute for Soldier Nanotechnologies at MIT, under Cooperative Agreement Number W911NF-18-2-0048. Micro-computed tomography instrumentation support by the Office of Naval Research (ONR) under grant number ONR.N000141712068 through the Defense University Research Instrumentation Program (DURIP) is gratefully acknowledged. This work was carried out in part through the use of MIT.nano's facilities.

## REFERENCES

[1] Salvetat, J. P., Bonard, J. M., Thomson, N. B., Kulik, A. J., Forró, L., Benoit, W., and Zuppiroli, L. "Mechanical Properties of Carbon Nanotubes." *Applied Physics A: Materials Science and Processing*, Vol. 69, No. 3, 1999, pp. 255–260. https://doi.org/10.1007/s003390050999.

[2] Zapata-Solvas, E., Gómez-García, D., and Domínguez-Rodríguez, A. "Towards Physical Properties Tailoring of Carbon Nanotubes-Reinforced Ceramic Matrix Composites." *Journal of the European Ceramic Society*, Vol. 32, No. 12, 2012, pp. 3001–3020. https://doi.org/10.1016/j.jeurceramsoc.2012.04.018.

[3] Squire, T. H., and Marschall, J. "Material Property Requirements for Analysis and Design of UHTC Components in Hypersonic Applications." *Journal of the European Ceramic Society*, Vol. 30, No. 11, 2010, pp. 2239–2251. https://doi.org/10.1016/j.jeurceramsoc.2010.01.026.

[4] Glass, D. (2008). Ceramic matrix composite (CMC) Thermal Protection Systems (TPS) and hot structures for hypersonic vehicles. *15th AIAA International Space Planes and Hypersonic Systems and Technologies Conference*. https://doi.org/10.2514/6.2008-2682

[5] Roewer, G., Herzog, U., Trommer, K., Müller, E., and Frühauf, S. "Silicon Carbide — A Survey of Synthetic Approaches, Properties and Applications." *High Performance Non-Oxide Ceramics I*, 2002, pp. 59–135. https://doi.org/10.1007/3-540-45613-9_2.

[6] Dai, J., Acauan, L., Jagani, S., Patel, P., Panova, V., & Wardle, B. L. (2023). Fabrication and characterization of carbon nanotube/Silicon Carbide nanocomposite laminates. *AIAA SCITECH 2023 Forum*. https://doi.org/10.2514/6.2023-2033

[7] Kaiser, A. L., Stein, I. Y., Cui, K., and Wardle, B. L. "Process-Morphology Scaling Relations Quantify Self-Organization in Capillary Densified Nanofiber Arrays." *Physical Chemistry Chemical Physics*, Vol. 20, No. 6, 2018, pp. 3876–3881. https://doi.org/10.1039/C7CP06869G.

[8] Stein, I. Y., Kaiser, A. L., Constable, A. J., Acauan, L., and Wardle, B. L. "Mesoscale Evolution of Non-Graphitizing Pyrolytic Carbon in Aligned Carbon Nanotube Carbon Matrix Nanocomposites." *Journal of Materials Science*, Vol. 52, No. 24, 2017, pp. 13799–13811. https://doi.org/10.1007/s10853-017-1468-9.

[9] Lee, J., Stein, I. Y., Devoe, M. E., Lewis, D. J., Lachman, N., Kessler, S. S., Buschhorn, S. T., and Wardle, B. L. "Impact of Carbon Nanotube Length on Electron Transport in Aligned Carbon Nanotube Networks." *Applied Physics Letters*, Vol. 106, No. 5, 2015, p. 053110. https://doi.org/10.1063/1.4907608.

[10] Stein, I. Y., and Wardle, B. L. “Morphology and Processing of Aligned Carbon Nanotube Carbon Matrix Nanocomposites.” *Carbon*, Vol. 68, 2014, pp. 807–813. https://doi.org/10.1016/j.carbon.2013.12.001.

[11] Stein, I. Y., and Wardle, B. L. “Coordination Number Model to Quantify Packing Morphology of Aligned Nanowire Arrays.” *Physical Chemistry Chemical Physics*, Vol. 15, No. 11, 2013, pp. 4033–4040. https://doi.org/10.1039/C3CP43762K.

[12] Stein, I. Y., and Wardle, B. L. “Packing Morphology of Wavy Nanofiber Arrays.” *Physical Chemistry Chemical Physics*, Vol. 18, No. 2, 2015, pp. 694–699. https://doi.org/10.1039/C5CP06381G.

[13] Kaiser, A. L., Chazot, C. A., Acauan, L. H., Albelo, I. V., Lee, J., Gair, J. L., Hart, A. J., Stein, I. Y., & Wardle, B. L. (2022). High-volume-fraction textured carbon nanotube–bis(maleimide) and −epoxy matrix polymer nanocomposites: Implications for high-performance structural composites. ACS Applied Nano Materials, 5(7), 9008–9023. https://doi.org/10.1021/acsanm.2c01212

[14] Poerschke, D. L., Braithwaite, A., Park, D., & Lauten, F. (2018). Crystallization behavior of polymer-derived si-O-C for ceramic matrix composite processing. Acta Materialia, 147, 329–341. https://doi.org/10.1016/j.actamat.2018.01.052

[15] Rao, A. M., Jorio, A., Pimenta, M. A., Dantas, M. S. S., Saito, R., Dresselhaus, G., and Dresselhaus, M. S. “Polarized Raman Study of Aligned Multiwalled Carbon Nanotubes.” *Physical Review Letters*, Vol. 84, No. 8, 2000, p. 1820. https://doi.org/10.1103/PhysRevLett.84.1820.

[16] See, A., Hassan, J., Hashim, M., Wahab, Z. A., Halim, D. N., Abdullah, M. S., & Azis, R. S. (2016). Dielectric behavior of β-sic nanopowders in air between 30 and 400 °C. *Journal of Materials Science: Materials in Electronics*, *27*(7), 6623–6629. https://doi.org/10.1007/s10854-016-4608-0

[17] Oliver, W. C., and Pharr, G. M. “An Improved Technique for Determining Hardness and Elastic Modulus Using Load and Displacement Sensing Indentation Experiments.” *Journal of Materials Research*, Vol. 7, No. 6, 1992, pp. 1564–1583. https://doi.org/10.1557/JMR.1992.1564.

[18] Al-Ajrash, S. M. N., Browning, C., Eckerle, R., and Cao, L. “Innovative Procedure for 3D Printing of Hybrid Silicon Carbide/Carbon Fiber Nanocomposites.” *Nano Select*, Vol. 2, No. 11, 2021, pp. 2201–2208. https://doi.org/10.1002/NANO.202100011.

[19] Gladstein, A. “Visualization and Analysis of Nanoscale Microstructure Evolution of In Situ Metal Matrix Composites.” 2022. https://doi.org/10.7302/6194.

[20] King, D., Apostolov, Z., Key, T., Carney, C., & Cinibulk, M. (2017). Novel processing approach to polymer-derived ceramic matrix composites. International Journal of Applied Ceramic Technology, 15(2), 399–408. https://doi.org/10.1111/ijac.12805